Fault reactivation and rift localization: Northeastern Gulf of Aden margin

N. Bellahsen,[1,2] M. Fournier,[3] E. d'Acremont,[3] S. Leroy,[3] and J. M. Daniel[1]

Received 20 January 2004; revised 28 October 2005; accepted 21 November 2005; published 17 February 2006.

[1] The Gulf of Aden and the Sheba spreading ridge (Gulf of Aden) forms the southern boundary of the Arabian Plate. Its orientation (075°E) and its kinematics (about 030°E divergence) are interpreted as the result of an oblique rifting. In this contribution, a field study in the northeastern Gulf of Aden allows us to confirm the Oligo-Miocene synrift directions of extension and to precise the normal fault network geometry. The synrift extensions are 020°E and 160°E (possibly in this chronological order); the normal faults strike 070°E, 090°E, and 110°E. The results show that some characteristics are consistent with oblique rifting analogue models, while some others are not. Especially, fault reactivation of Mesozoic structures is shown to have occurred significantly at the beginning and during rifting. These data are therefore compared to analogue models of oblique reactivation, and this comparison demonstrates that fault reactivation played a key role during the early stage of the Gulf of Aden rifting. Finally, scenarios of the lithospheric evolution during the eastern Gulf of Aden opening (preexisting weaknesses in the lithosphere or not) are discussed to better constrain the deformation history of the northern margin. Especially, we show that rift localization processes may imply stress rotations through time.

Citation: Bellahsen, N., M. Fournier, E. d'Acremont, S. Leroy, and J. M. Daniel (2006), Fault reactivation and rift localization: Northeastern Gulf of Aden margin, *Tectonics*, *25*, TC1007, doi:10.1029/2004TC001626.

1. Introduction

[2] The Gulf of Aden is the southern boundary of the Arabian Plate (Figure 1). In the eastern part of the gulf, the oceanic basin currently opens at a rate of 2.2 cm/yr along a direction 025°E [*Jestin et al.*, 1994; *Fournier et al.*, 2001]. The opening started at 35 Ma [*Roger et al.*, 1989] with extension around 020°E (direction deduced from fault slip data, see below) in the rift striking 075°E. We will assume that the opening direction was 020°E to 025°E during rifting, i.e., similar to the present opening direction. This kinematics is consistent with an oblique rifting configuration, the angle α between the present opening direction and the rift orientation being 50°. The normal fault networks of the rift have been studied in many places along the margins, including Somalia [*Fantozzi and Sgavetti*, 1998], Yemen [*Huchon and Khanbari*, 2003], and Oman [*Lepvrier et al.*, 2002; *Fournier et al.*, 2004]. They were interpreted as the consequence of the oblique rifting. These field studies showed that the fault network is intensively segmented and fault orientations are very scattered. Moreover, several directions of extension are recorded in Yemen [*Huchon et al.*, 1991; *Khanbari*, 2000; *Huchon and Khanbari*, 2003] and in Oman [*Lepvrier et al.*, 2002]. In Yemen, a 020°E extension is shown to predate a 160°E extension [*Huchon et al.*, 1991; *Khanbari*, 2000; *Huchon and Khanbari*, 2003], whereas in Oman the chronology is less obvious [*Lepvrier et al.*, 2002; *Fournier et al.*, 2004]. In this paper, we present new field data on fault geometries and orientations, and undertake a new paleostress study that compliments the ones cited above.

[3] The origin of the oblique rift orientation is not well understood. Models of oblique rifting require a preexisting lithospheric discontinuity that localizes the rift obliquely relatively to the displacement direction. While some authors proposed Pan-African lineaments [*Berhe*, 1986; *Katz*, 1987] or hot spot tracks [*Morgan*, 1983], it is not demonstrated that such heterogeneity has influenced the rifting. The opening of the Gulf of Aden is then often seen as the WSW propagation of the Carlsberg ridge (Northwest Indian ocean) in the direction of the Afar hot spot [*Courtillot*, 1980; *Courtillot et al.*, 1987; *Manighetti et al.*, 1997], a mechanism generalized in *Courtillot et al.* [1999]. The propagation of the ridge in the gulf was seen as episodic with stops at the main transform zones. However, no rift propagation is recorded in the sediments along the margin. The rifting onset is dated around 35 Ma; however, the age of the magnetic anomalies is at least 17.6 Ma [*Leroy et al.*, 2004; *d'Acremont et al.*, 2006]. The propagation of the Aden ridge is clear in the western part of the gulf where it enters the Tadjoura Gulf toward Afar [*Manighetti et al.*, 1998; *Dauteuil et al.*, 2001]. Recently, *Jolivet and Faccenna* [2000] and *Bellahsen et al.* [2003] proposed that this kinematics (direction and extension in the Gulf of Aden rift) was due to the interaction of the boundary conditions of the incipient Arabian Plate and the presence of the Afar hot spot. The progressive transition from oceanic to continental subduction along the Bitlis-Zagros-Makran convergence zone triggered, around 35Ma, intraplate extensive stresses

[1]Institut Français du Pétrole, Rueil Malmaison, France.
[2]Now at Laboratoire de Tectonique, Université Pierre et Marie Curie, Paris, France.
[3]Laboratoire de Tectonique, Université Pierre et Marie Curie, Paris, France.

0278-7407/06/2004TC001626$12.00

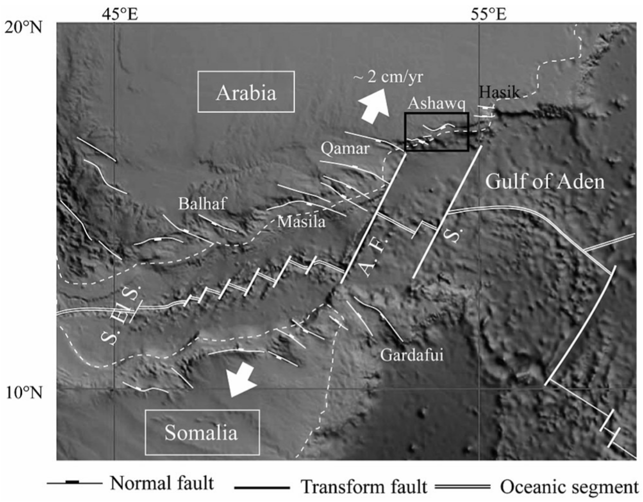

Figure 1. Simplified structural map of the entire Gulf of Aden. The mid-oceanic ridge is the boundary between the Arabian Plate and the Somalian Plate. The major basins and faults are shown. Their orientations are around 110°E, while the gulf axis is around 075°E. These structures are arranged en échelon along the margin with a long overlap between them. The gulf currently opens at a rate of about 2 cm/yr in a direction 027°E [*Jestin et al.*, 1994] to 033°E [*Fournier et al.*, 2001]. Five mains basins are recognized on the northern margin. On the southern, only one is identified (the Gardafui basin [see *d'Acremont et al.*, 2005]). A.F. is the Alula Fartak transform fault, S. is the Socotra transform fault, and S. El S. is the Shukra El Sheik discontinuity. The studied area is located in the black rectangle.

in the African plate. The dynamics of the Afro-Arabian rifts have been reproduced in laboratory without any lithospheric weakness, except the Afar hot spot [*Bellahsen et al.*, 2003]. This result implies a different evolution than in a classical oblique rift.

[4] The second important parameter that is discussed here is the presence of preexisting faults. It is well known that Mesozoic tectonic events have created numerous normal faults and basins in the Arabian platform. These basins were reactivated during the Tertiary rifting, especially in Yemen [*Khanbari*, 2000; *Granath*, 2001]. Thus we hypothesize that fault reactivation also occurred in Oman. Another kind of fault reactivation should also be taken into account. If the extension changes orientation during rifting, for example from 020°E to 160°E, active faults during the first phase could be obliquely reactivated during the second phase. Thus, in this paper, we will apply some analogue model results, published in a separate paper [*Bellahsen and Daniel*, 2005], to the Gulf of Aden.

[5] Finally, we address the question of the origin of the 160°E extension that is recorded along the entire Gulf of Aden. *Huchon and Khanbari* [2003] proposed a crack tip propagation model in which the extension 160°E is due to the WSW propagation of the Aden ridge during the Miocene. An alternative model will be proposed here, taking into account the lithospheric evolution of an oblique rift, whose obliquity is not due to a preexisting lithospheric discontinuity.

2. Geological Setting

[6] The geological history of the present Arabian plate started in Neo-Proterozoic times with the formation of two N-S sutures in western Arabia (Nabitah and Amar sutures) [*Al-Husseini*, 2000]. At the Proterozoic-Paleozoic transition, extensional events created N-S to 045°E trending rifts (Oman and Dibba rifts) accompanied by large strike slip faults trending 110 to 130°E (Nadj Fault Zones) [*Al-Husseini*, 2000]. At the end of the Jurassic and the beginning of Cretaceous, the Africa-Madagascar separation created E-W to 110°E basins and normal faults, particularly around Socotra island [*Birse et al.*, 1997] and in Yemen [*Beydoun et al.*, 1996; *Birse et al.*, 1997; *Bosence*, 1997; *Khanbari*, 2000].

[7] During late Cretaceous, a transgression occurred in Dhofar [*Platel and Roger*, 1989; *Roger et al.*, 1989] and thick limestone and shale-limestone formations were deposited. A regression from late Cretaceous triggers the Dhofar emersion during the Paleocene. In Eocene times, thick limestone sequences (around 800 m) were unconformably deposited over the upper Maastrichtian formations.

[8] Synrift sedimentation started around 35 Ma in Oman [*Roger et al.*, 1989] and in Yemen [*Watchorn et al.*, 1998]. The synrift formations show a transgression during Oligocene, while during Miocene times, a regression marks the final uplift of the margin. However, a final marine incursion occurred and the postrift Adawnib formation is dated at 18 Ma [*Roger et al.*, 1989]. In Yemen, the postrift base is dated between 21.1 and 17.4 Ma from strontium isotope dating [*Watchorn et al.*, 1998].

3. Field Data

3.1. Fault and Synrift Basin Geometries

[9] The basins and active normal faults during the Oligo-Miocene rifting have several directions mainly around 070°E, E-W and 110°E and are arranged en échelon, along the margin that has a trend at about 075°E (Figures 1 and 2). The faults are composed of segments of various orientations and are classically interpreted as the consequence of the rifting obliquity. Several grabens can be identified and the most important is the Salalah plain–Ashawq Graben where the synrift largely crops out. This basin was controlled by a fault composed of segments of various strikes: from west to east, 110°E, 070°E and, 110°E. In the Salalah plain, a postrift unit covers the synrift sequence, as these synrift sediments did probably not fill the space available in this graben. Maximum hanging wall subsidence was probably located beneath the Salalah plain near the intersection between segments striking 070°E and 110°E (north of Salalah, Figures 2 and 3). Furthermore, local uplift maximum was probably located at the other intersection (north of Mughsayl). Especially in the western part, Cretaceous (and Paleozoic) rocks crop out in the footwall (Figures 2 and 3). These outcrops suggest a high rate of erosion certainly related to a high rate of local uplift due to the faults.

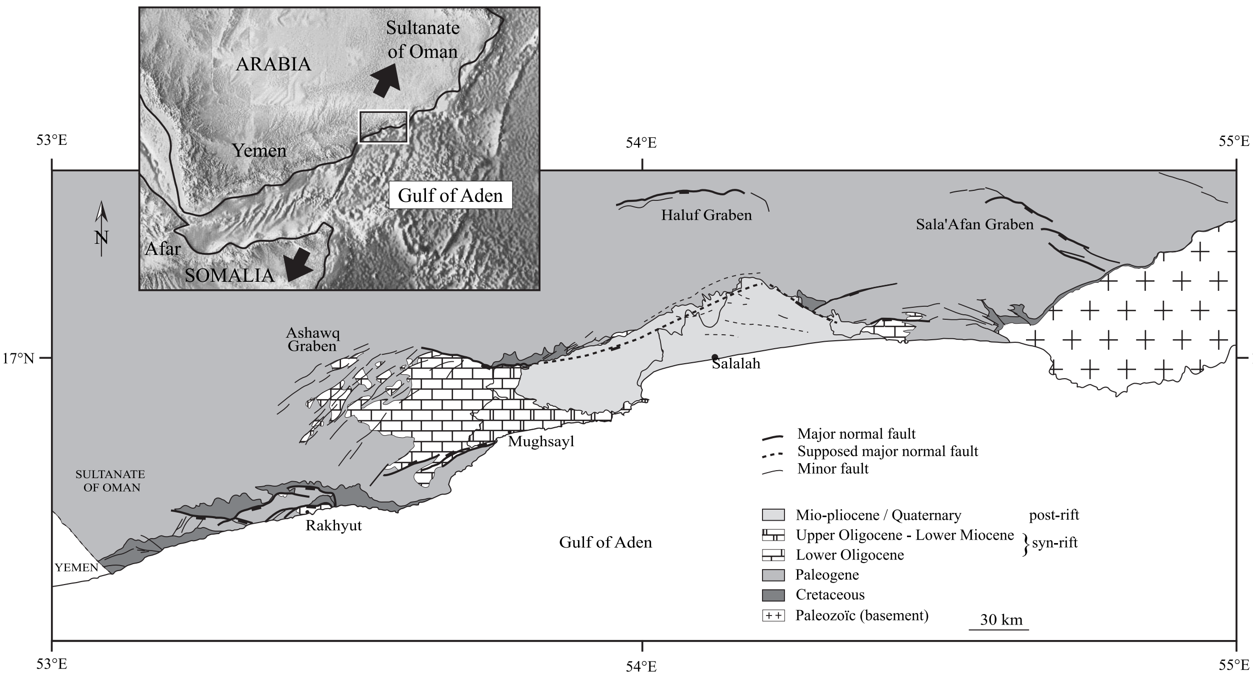

Figure 2. Geological and structural map of the Dhofar (Oman) northeastern margin of the Gulf of Aden, from geological maps, field and satellite data (this study), and from *Roger et al.* [1989] and *Platel and Roger* [1989]. Note the various strikes of faults, their undulating trace, and the complex geometry of the basins. The synrift deposits are mainly located in the Salalah plain and Graben Ashawq. A few outcrops can be found in the Rakhyut and Haluf basin, whereas in the Sala'Afan, no synrift sedimentation is observed.

[10] To complete the geological maps, we interpreted SPOT images of the area, especially in the western part of the Ashawq Graben (Figure 4). On the satellite image, only the visible structures at the western tip of the border fault were mapped as faults. The interpretation is thus not exhaustive, but only used to highlight fault reactivation as outlined below and to build the structural map (Figure 2). At the western tip of the major fault of the Ashawq Graben (Figure 4), a network of normal faults has been mapped and documented in the field. Field investigation allows us to characterize slip that is purely normal. The fault lengths are from hundreds of meters to a few kilometers and throw is on the order tens to hundreds of meters. These faults are distributed across an area of 20 km by 20 km, at the vicinity of the border fault tip. Orientation varies from 070°E close to the major fault to 030°E further west. This geometry can be explained as horsetail geometry and this interpretation requires an oblique reactivation with left-lateral slip along the border fault [e.g., *Schlische et al.*, 2002].

[11] A few outcrops of synrift sediments are also found in the small Rakhyut basin, in the southwest part of the Dhofar area (Figure 2). This basin is controlled by faults with various strikes, from 070°E to 120°E. Two faults (fault A 100°E and fault B 070°E) intersect in this area (Figure 5) and, at their intersection in the footwall, Cretaceous sediments outcrop. Further east in the same area, 070°E faults (faults named C) that are recognized onshore continue offshore [*d'Acremont*, 2002; *d'Acremont et al.*, 2005] with a strike of about 110°E

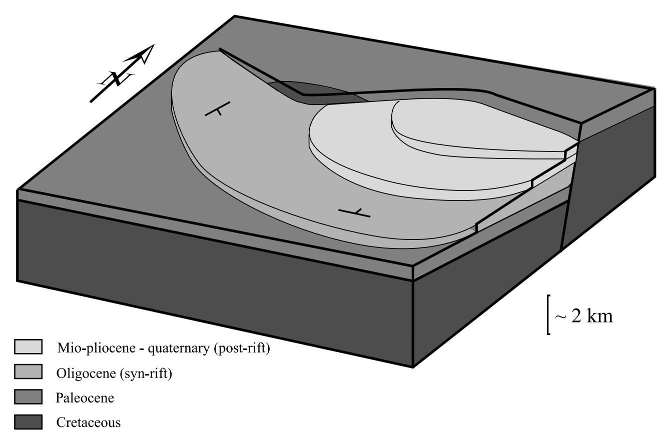

Figure 3. Simplified 3-D structure of the Salalah-Ashawq basin. The fault orientation varies along strike, from 110°E to the west, to 070° and 110°E again to the east. The bedding dire actions are strongly noncylindrical and the synrift thickness decreases westward, toward the basin extremity. While it increases eastward, the deepest depocenter is located at the eastern intersection of 110°E and 070°E fault segment. At the western intersection, some Mesozoic layers widely outcrops and suggest a zone of uplift. See text for explanation and discussion.

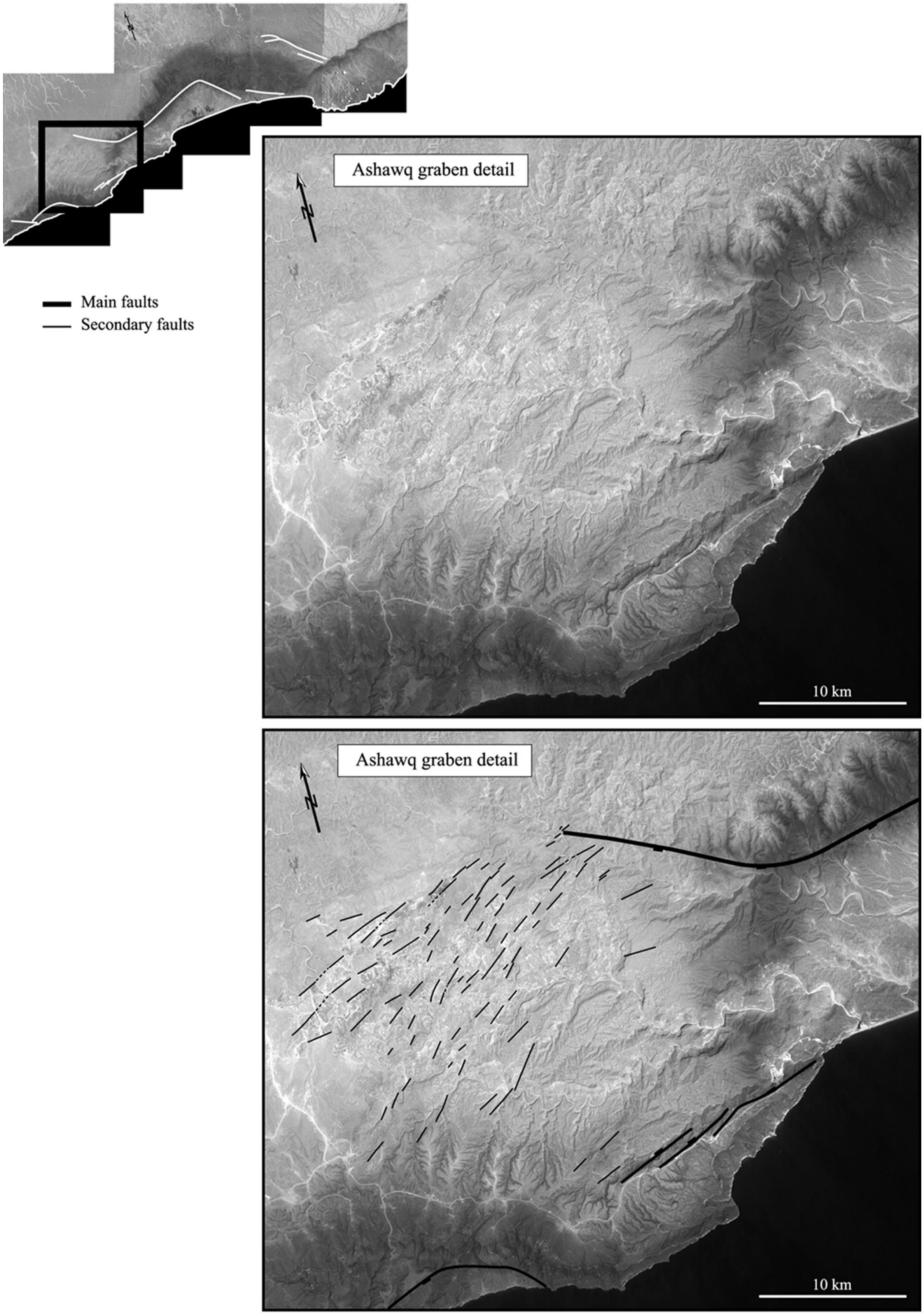
Main faults
Secondary faults
Ashawq graben detail
10 km
Ashawq graben detail
10 km

Figure 4

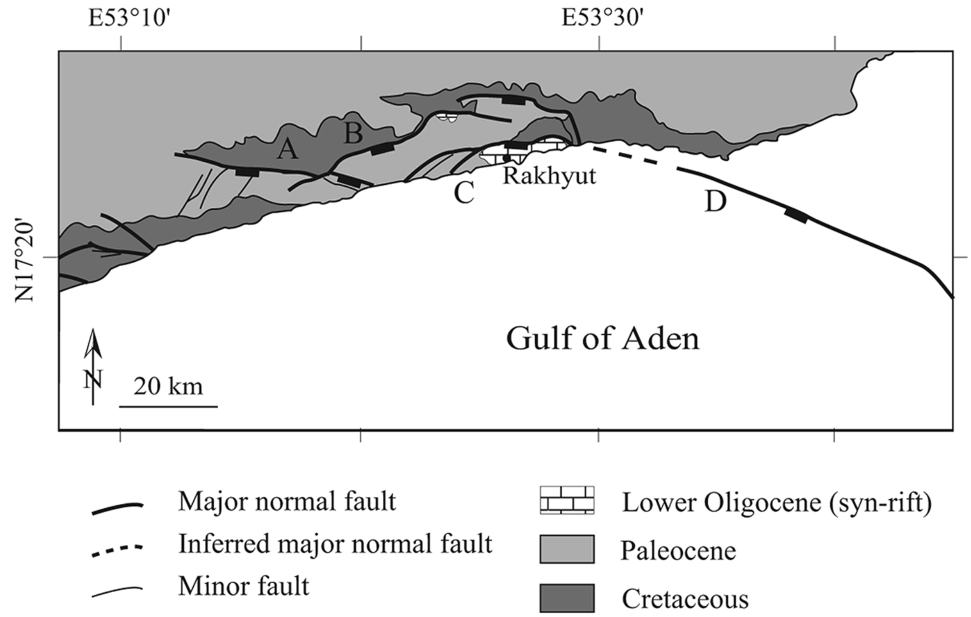

Figure 5. Zoom on the Rakhyut basin. The onshore faults can be extended offshore by a 110°E fault [*d'Acremont et al.*, 2005]. Some characteristics are similar to the ones of the Salalah-Ashawq Graben and discussed in the text. This is one of the basins where synrift deposits crop out, but are very limited. The fault is composed by 070°E to 110°E segments and the depocenter seems located at their intersection.

(fault D). At their intersection, in the hanging wall, a synrift basin is present, while synrift sediments are missing elsewhere in the area. Such geometry is similar to the one described for the Ashawq-Salalah basin at smaller scale.

[12] In the Haluf basin (Figure 2), the base of the synrift sequence can be observed and is controlled E-W normal faults that turn toward a 070°E strike in the western part. Finally, one graben lacking synrift sedimentation is recognized: the Sala'Afan graben (Figure 2) controlled by 110°E normal faults that strike 070°E at the western extremity. This geometry is compatible with an oblique left-lateral reactivation of 110°E segments that end as horse tail. Unfortunately, we do not have kinematic indicators on the fault planes to constrain this hypothesis in the Dhofar area. However, a left-lateral oblique reactivation of such structures seems to indicate that they might have been reactivated by the 160°E extension for kinematic consistency. All the characteristics of the normal faults described by the field data are discussed below.

[13] Several 070°E striking faults (rift axis parallel) are observed along the margin. However, these faults are mainly found in the external parts of the margin. It is shown, by *d'Acremont* [2002] and *d'Acremont et al.* [2005], that very few 070°E faults are present in the internal part of the margin (i.e., near the continent-ocean transition). These characteristics will be compared to analogue models of oblique rifting and oblique reactivation.

3.2. Paleostress Data

[14] Several paleostress tensors have been calculated and the orientations of the principal stresses are presented here. The method we used, along with its assumptions and limitations, are presented by *Angelier* [1984, 1989, 1990]. It is based on the collection of fault slip data sets. These tensors compliment the ones presented by *Huchon et al.* [1991], *Khanbari* [2000], *Lepvrier et al.* [2002], *Huchon and Khanbari* [2003], and *Fournier et al.* [2004]. In the area of Mughsayl (Figure 6), directions of extensions at 160°E, N-S and, 020°E are recorded in the upper synrift sequence. These extensions are characterized by 070°E, E-W and, 110°E striking dip-slip normal faults, respectively. In the western part of the area, at the western extreme of the Ashawq Graben (Figure 6), extensions a bit more oblique are observed: the directions are 130°E to 160°E. These extensions are characterized by dip-slip 040°E to 070°E striking normal faults. In the vicinity of the Ashawq Graben's northern border fault tip (Figure 6), extension around 150°E is recorded. This extension is deduced from dip-slip 060°E striking normal faults and from oblique-slip 110°E striking faults.

Figure 4. Spot images of the Graben Ashawq and structural interpretation. The major fault is drawn (thick lines). Minor normal faults are also highlighted (thin lines) and are mapped from lineaments, field observation and texture differences between the synrift and anterift sediments. This structure is very similar to a horsetail configuration and suggests a left-lateral slip component on the major fault. However, few oblique slickenlines are found in the field, mainly because of outcrop quality.

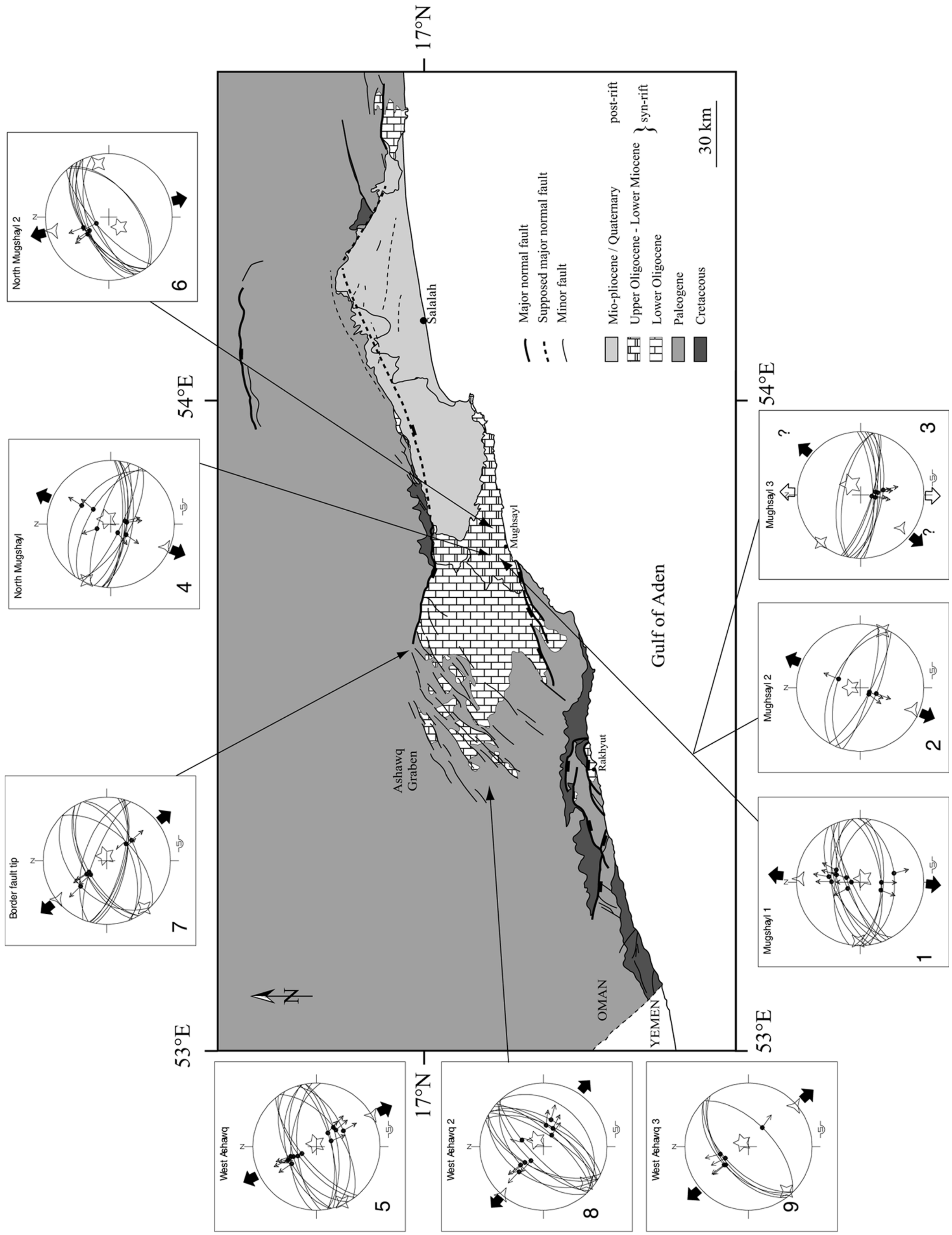
17°N
54°E
53°E
Salalah
Mughsayl
Rakhyut
Ashawq Graben
Gulf of Aden
OMAN
YEMEN
Major normal fault
Supposed major normal fault
Minor fault
Mio-pliocene / Quaternary
Upper Oligocene - Lower Miocene
Lower Oligocene
Paleogene
Cretaceous
post-rift
syn-rift
30 km
North Mugshayl 2
North Mugshayl
Border fault tip
West Ashawq
West Ashawq 2
West Ashawq 3
Mughsayl 1
Mughsayl 2
Mughsayl 3

Figure 6

[15] These results mainly show dip-slip movement on normal faults. They show, only in one case, oblique slip on segments striking 110°E, with an extension direction of 160°E (Figure 6, site 7). These data thus do not allow us to constrain the chronology of the 020°E and 160°E extension directions, nor to infer oblique reactivation of fault segments. However, these results are consistent with previous studies [*Huchon et al.*, 1991; *Khanbari*, 2000; *Lepvrier et al.*, 2002; *Huchon and Khanbari*, 2003]. Huchon and coworkers showed that the 020°E extension direction seems to predate the 160°E extension. These results are consistent with the fact that the 020°E direction is in the kinematic direction of plate divergence. This first stage of extension can be generated by boundary conditions that are discussed by *Bellahsen et al.* [2003]. The 160°E extension could then be due to a "local" stress perturbation whose origin will be discussed later. In the following, we will assume this chronology (020°E extension followed by 160°E) as a working hypothesis. However, as the causes for these extensional phases are still under debate, we present another set of data composed of fault orientation distributions, which are often used to determine the rift kinematics [*Tron and Brun*, 1991; *Brun and Tron*, 1993; *Dauteuil and Brun*, 1993; *Dauteuil et al.*, 2001].

3.3. Fault Orientation Distribution

[16] The structural map (Figure 2) shows complex fault geometries. The faults are composed of several segments of different orientations. For example, the major normal fault of the Salalah plain and Ashawq Graben is very sinuous, like the faults of the Rakhyut area. This fault network's segmentation is also clearly visible on the fault orientation frequency diagram (Figure 7). These diagrams are constructed for different kind of faults: for major and minor faults of the structural map, i.e., main faults (Figure 7a) and for faults strikes measured in the field, i.e., small faults (Figure 7d). For the first two data sets, where the length is known, the frequency is weighted according to the fault length.

[17] The diagram of the main faults (Figure 7a) shows three frequency peaks: one peak between 060°E and 080°E, one between 090°E and 100°E, and one between 105°E and 120°E. The first peak therefore represents faults striking parallel to the rift axis (around 075°E), the third peak the faults subperpendicular to the plate divergence (025°E). The second peak represents faults that have an intermediate orientation, i.e., between the rift axis and normal to the divergence (called faults of intermediate direction).

[18] The small faults (Figure 7d) show a more complex distribution of orientation. We see the fault population between 060°E and 120°E, as in the plot of the large faults. In this range, it is difficult to separate distinct fault populations. We also see several faults striking between 020°E and 055°E. The complexity of this diagram can be explained by the fact that these faults are secondary structures and initiate in the vicinity of larger faults that perturb the stress field and thus the orientation of new faults. Stress perturbations (in magnitude and in orientation) especially occur in cases of oblique fault reactivation. The 020°E–055°E fault population is particularly observed in the western part of the Ashawq Graben (Figure 2) and comprises the horsetail described in section 3.1.

4. Discussion

[19] Along the northeastern margin of the Gulf of Aden, two synrift extensions are recorded, 020°E and 160°E. The normal fault network is complex, segmented, and composed of several fault populations having strikes 070°E, E-W and, 110°E. This section discusses the possible origins for these geometries and kinematics.

4.1. Influence of the Rift Obliquity

[20] In case of oblique rifting, *Withjack and Jamison* [1986] show analytically and in analogue models that displacement (or opening direction) and direction of extension are not parallel. In the Gulf of Aden (striking 075°E), the extension directions are around 020°E, N-S and 160°E. The opening direction at rifting times is unknown and the present one is around 025°E. We here investigate the case of an oblique rifting with an angle α of 45° (α is the angle between the rift orientation and the opening direction).

[21] The fault orientation plot for large faults (Figure 7a) shows several frequency peaks. Two of these peaks are well predicted in analogue models of oblique rifting by *Tron and Brun* [1991] (Figure 7b). In these models, where the angle α is equal to 45°, the peaks of faults parallel to the rift axis and of intermediate direction are effectively observed; in the models as well as in the Gulf of Aden, one population trends at around 75–80° to the direction of divergence. Another population trends at approximately 50° to the direction of divergence and is rift parallel. Moreover, as explained earlier, the faults parallel to the rift axis are present only in the external part of the rift and are not observed offshore [*d'Acremont et al.*, 2005] near the continent-ocean transition. This is also consistent with analogue models where these faults are border faults (here referring to the faults at the margin of the deformed zone, see Figure 3 of *Tron and Brun* [1991] or of *McClay and White* [1995]). However, these faults are clearly less numerous in the models than in the margin, which could be a scale effect. Moreover, this population is even less represented in the analogue models of *Withjack and Jamison* [1986] and *Clifton et al.* [2000] (Figure 7c). They are actually not

Figure 6. Paleostress inversion of fault slip data using the method of *Angelier* [1989]. The data are located in the western part of the studied area. The stress fields are highly heterogeneous, with directions from 135°E to 020°E and intermediate orientations. In the western part of the Salalah-Ashawq graben, 135°E to 150°E extension directions are found. Eastward, 020°E and 160°E extension directions are found without evident chronology between them. White arrows are drawn when the inversion (black arrow) is clearly wrong (no conjugate faults with striae, site Mughsayl 3).

numerous enough to form a frequency peak, even if their number increases a bit with increasing strain. The differences between the *Tron and Brun* [1991] models and the *Clifton et al.* [2000] models are the materials (sand and clay, respectively) and their thickness and the basal conditions (velocity discontinuity vs. rubber sheet). In the *Tron and Brun* [1991] experiments, the sand is underlain by ductile silicone that does not extend from the mobile wall to the other. The axis-parallel faults initiate in the area of the silicone boundary. This may explain the presence of a peak at this direction and its absence in the other models. In the *Clifton et al.* [2000] models, the clay is directly above the rubber sheet. In this case, no axis-parallel faults initiate. In the work by *McClay and White* [1995], these faults are also less numerous and the sand directly covers the rubber sheet.

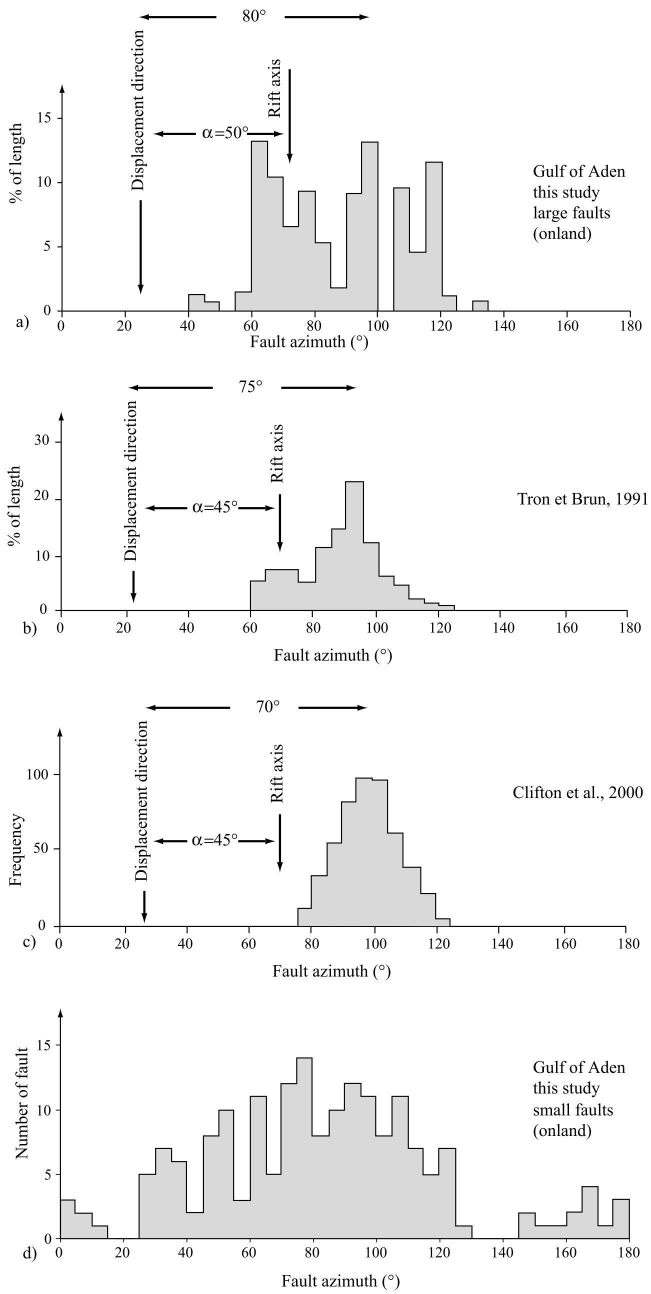

[22] In summary, the analogue models do not predict one of the fault populations, i.e., the faults striking 110°E perpendicular to the divergence direction (020°E). In analogue models of oblique rifting (whatever the rift obliquity), mainly faults with strike intermediate between the perpendicular to the divergence and the rift axis initiate (as analytically and experimentally highlighted and explained by *Withjack and Jamison* [1986]). Therefore the published analogue models of oblique rifting predict several characteristics of oblique rifts and greatly help us to interpret fault networks. However, to apply them to the Gulf of Aden, one must consider other parameters (that are listed below) that may explain the differences between the field data and the models.

[23] Three scenarios are hypothesized. First, the presence and the reactivation of 110°E preexisting faults during the early phases of the rifting could explain the presence of these 110°E faults. This explanation invokes some crustal complexities to explain the observed geometries. The rifting mechanism is then, in this case, an oblique rifting with preexisting faults perpendicular to the divergence. Second, we could invoke a rift mechanism with a first period of orthogonal rifting and then a period of oblique rifting. In such case, the orthogonal rifting period (divergence 020°E) generates (and/or reactivates) 110°E faults and the oblique rifting overprints the previous structures. Third, stress rotations during the rifting could produce fault reactivation of earlier faults. These two last explanations deal with the behavior of the whole lithosphere and rift localization processes that will be discussed further.

4.2. Influence of Oblique Fault Reactivation

[24] To take into account the reactivation, analogue models of oblique fault reactivation are presented here. These models are described in more details in another paper [*Bellahsen and Daniel*, 2005]. The main results are briefly summarized here for comparison to the fault geometry of the Gulf of Aden.

Figure 7. Distribution of fault segment orientation. (a) Distribution of the percentage of fault length vs. their azimuth. This diagram plots faults, whose length can be measured, i.e., mainly geologically mapped faults from the satellite interpretation. The angle (80°) is the angle between the opening direction and the main fault population as in Figures 7b and 7c. The angle α is the angle between the opening direction and the rift axis. (b) Distribution of fault orientation in analogue models of oblique rifting of *Tron and Brun* [1991] for a kinematic context similar to the one of the Gulf of Aden (angle between the rift orientation and the opening direction, α, equal to 45°). Note the differences between the data at around 110°E (see text for discussion). (c) Distribution of fault orientation in analogue models of oblique rifting (angle α equal to 45°) of *Clifton et al.* [2000]. Only one peak is recorded. (d) Distribution of fault segments whose length cannot be measured, i.e., field measurements of fault orientation.

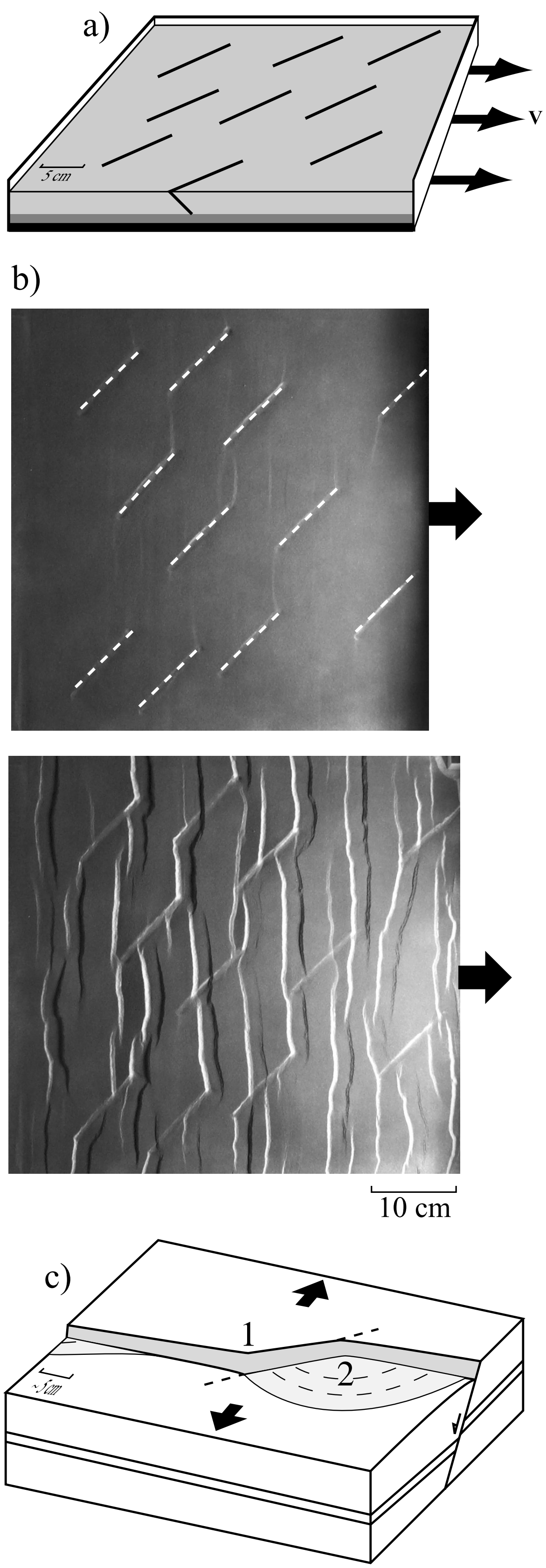

Figure 8. Analogue models of fault reactivation from *Bellahsen and Daniel* [2005]. (a) Model setup. (b) Results. The faults are composed of reactivated and newly created segment and show characteristic geometries. (c) Conceptual 3-D model of a relay zone where the relay fault is a reactivated one. The topography, the location of depocenters and the kinematics are characteristic. Especially, at intersection 1, the uplift is maximum in the footwall, and at intersection 2, the subsidence is maximum in the hanging wall.

[25] As shown in the previous sections, at least two extension directions are recorded on the margins of the Gulf of Aden: an extension with a 020°E direction and a 160°E extension. In some places in Yemen and Oman, the 020°E seems to predate the 160°E [*Huchon et al.*, 1991; *Khanbari*, 2000; *Lepvrier et al.*, 2002; *Huchon and Khanbari*, 2003]. Normal faults, active during the first extension and striking 110°E, may be reactivated obliquely during the second extension (160°E) as suggested by field observations (section 3). Analogue models of oblique reactivation can help us to study this phenomenon. The analogue models are made of sand representing brittle layers (2 cm) and silicone putty representing ductile layers (1 cm) (Figure 8a) deformed by stretching of a basal rubber sheet. These materials have been repeatedly used for modeling the brittle and ductile deformation of the crust; the experiments are scaled down to nature [e.g., *Hubbert*, 1937; *Davy and Cobbold*, 1991] and the scaling factors are given by *Bellahsen and Daniel* [2005]. The discontinuities are zones of dilation, trending at 45° to the direction of divergence, in which the coefficient of friction is decreased. These discontinuities are made before the extension, by introducing a cardboard along a dip of 60° and with a length of 10 cm.

[26] The discontinuities are reactivated (Figure 8b). They show a significant throw and propagate perpendicularly to the applied extension direction. However, they do not accommodate the whole applied extension (because of their orientations). The newly created faults and the propagated segments of the reactivated discontinuities (both subperpendicular to the extension) accommodate a great part of the applied extension. As a result, the faults are composed of reactivated segments and newly created ones (Figure 8b). They are thus much more segmented than faults created in homogeneous brittle layers. The elevation around these kinds of faults is characteristic. In the footwall, the maximum elevation occurs at one of the intersections (see location 1 on Figure 8c). In the hanging wall, the maximum subsidence occurs at the other type of intersection (see location 2 on Figure 8c).

[27] This fault pattern is similar to the one observed in our field data part. This configuration thus suggests an oblique reactivation of 110°E striking faults by an extension at 160°E, which also creates 070°E striking faults. However, two scenarios are possible:

[28] 1. The 110°E faults are preexisting (Figure 9a), reactivated during an 020°E extension phase, and propagate as dip-slip faults (Figure 9b). During the latter 160°E extension phase, they are obliquely reactivated contemporaneously with the creation of 070°E segments (Figure 9c).

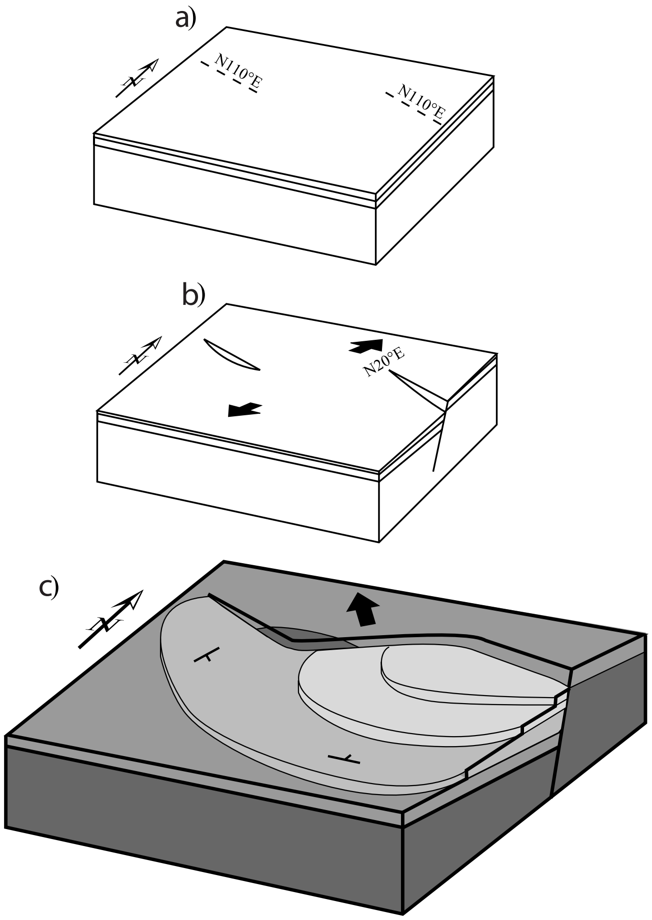

Figure 9. Interpretation of the Salalah-Ashawq Graben structure. (a) Hypothetical situation of the area before rifting. (b) Reactivation or creation of the 110°E faults during the 020°E extension phase. (c) Simplified 3-D structure of the Salalah-Ashawq Graben and kinematics during the 160°E extension. See text for explanation.

In this scenario, reactivation occurred orthogonally at the beginning of the rifting and obliquely during the rifting.

[29] 2. The 110°E segments are created during the 020°E extension phase (Figure 9b) and are obliquely reactivated during the 160°E extension (Figure 9c). In this scenario, reactivation occurred only obliquely during rifting. However, the resulting geometry should be the same and the 3-D geometrical characteristics only constrain the last oblique reactivation event.

[30] These observations, field data (fault geometry, horse tails, paleostresses, orientation distribution), and results of analogue models, indicate that reactivation processes occurred during the Oligocene rifting of the Gulf of Aden in Oman and confirm the hypothesis of a 020°E extension followed by a 160°E extension.

4.3. Reactivation of Mesozoic Basins

[31] As shown by *Khanbari* [2000] in Yemen and *Ellis et al.* [1996] in the whole Gulf of Aden, the Oligocene rifting of the Gulf of Aden reactivates older basins active during the Cretaceous rifting. These Cretaceous basins are oriented E-W to 110°E and thus subperpendicular to the early 020°E extension during Oligocene times. These basins are en échelon along the Gulf of Aden margins with very large overlaps between basins (Figure 1). This pattern tends to show that these basins are inherited from previous extensional events and not driven by rift obliquity.

[32] On the contrary, in analogue models of oblique rifting (in homogeneous brittle layer) (Figure 10a), the basins are initiated during rifting and their geometry depends on the obliquity [*McClay and White*, 1995]. In this case, they are characterized by shorter overlapping zones. The deformation between two adjacent basins is transferred along accommodation zone. In such cases, the oceanization process may occur in the basin center, where extension is the higher. The very largest accommodation zones may evolve in major transform faults (first-order transform faults, such as the Alula Fartak transform fault). In this case, we can extrapolate the rift geometry of *McClay and White* [1995] as shown in Figure 10b.

[33] In the case of inherited basins, the rift obliquity does not control the basin disposition. At the onset of accretion, the transform zones cannot simply be located at the extremities of each basin without cutting another basin. The oceanic segments cannot localize in all the sedimentary basins. Looking at the gulf closed at the anomaly 5c [*d'Acremont et al.*, 2005, 2006], the Gardafui basin has a similar orientation (well defined in bathymetric map, Figure 1) as the Qamar basin and actually corresponds to the offset eastern part of the Qamar basin (Figure 10c). The Qamar/Gardafui basin was cut by the Alula Fartak transform zone. No oceanic spreading occurred in this basin that has been offset by the transform fault. This highlights the particular location of transform fault zones in oblique rifting with preexisting basin disposition. Some oceanic spreading are then located in rifted basins while another are abandoned during the oceanization process.

4.4. Lithospheric Thinning

[34] At the scale of the whole lithosphere, the behavior of its mantle part has to be taken into account, assuming that the location of the high lithospheric strength is located in this layer [e.g., *Brun*, 1999]. We argued earlier that the lithospheric mantle in the eastern Gulf of Aden was not locally weakened before the Oligocene rifting. However, the two cases (weaken and unweakened lithospheric mantle) must be discussed.

4.4.1. Weaken Lithospheric Mantle

[35] Let us first assume that the lithospheric mantle was weakened as it is generally assumed in oblique rifting context (and sometimes demonstrated as in the Viking Graben for example [*Brun and Tron*, 1993; *Faerseth et al.*, 1997]). Zones of weakness are present both in the crust and in the mantle lithosphere: in the Gulf of Aden, the rift would have localized along the lithospheric mantle weakness (075°E) and the extension (due to the divergence 020°E) in the crust would be accommodated in reactivated preexisting basins and faults oriented around 110°E. Such a

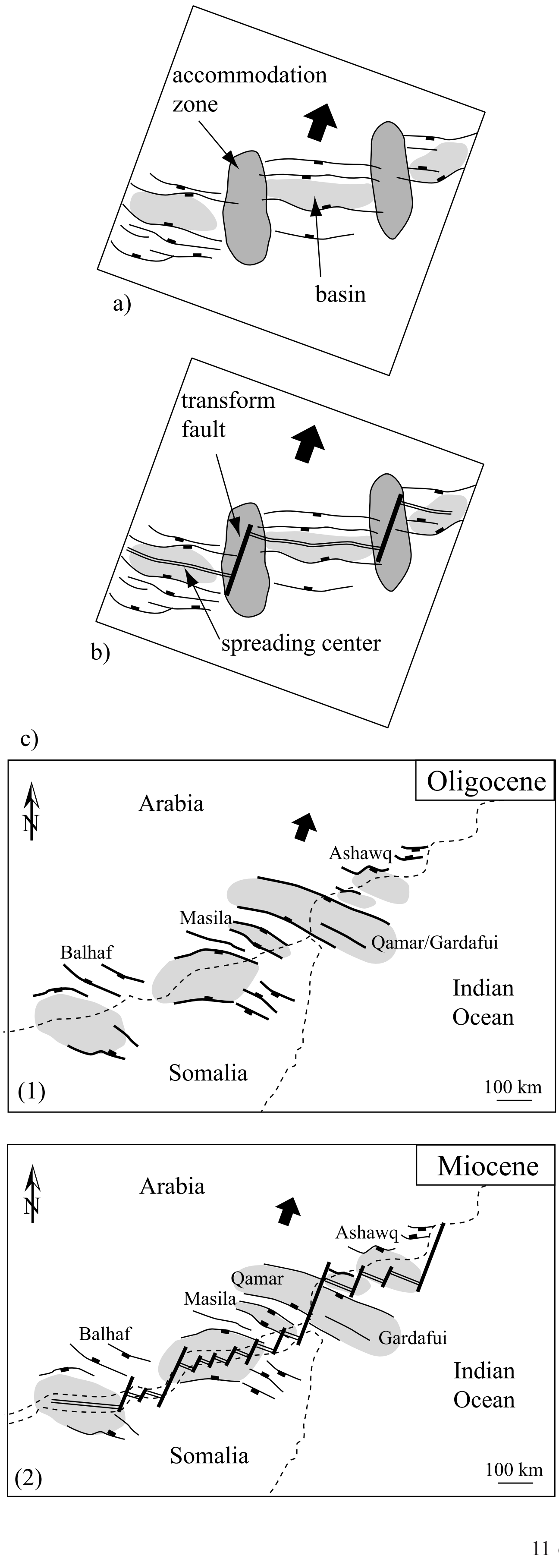

Figure 10. Evolution of oblique rifts. (a) After *McClay and White* [1995]. (b) Our extrapolation of a possible oceanic evolution of such an oblique rift. The spreading center would localize in the basins, the transform faults in the accommodation zones. (c) Simplified and idealized situation of the eastern Gulf of Aden. Note the differences in basin overlaps and transform locations; specially, the Alula-Fartak transform zone is located and cut the large Qamar-Gardafui basin. Sketch of oceanic basin modified from *Leroy et al.* [2004] and *d'Acremont et al.* [2005].

scenario can explain the fact that we observe 110°E faults not predicted by analogue models of oblique rifting. This scenario was one of the hypotheses made in earlier sections, an oblique rifting with inherited faults perpendicular to the divergence. The obliquity of the rifting also created faults of direction (E-W) intermediate between the perpendicular to the extension (110°E) and the rift axis (075°E), as predicted by analogue models and measured in the field. In such a case, the obliquity was established from the onset of rifting and thus a situation of a "real and classical" oblique rift. The weakness in the lithosphere that localized the rift axis should have induced a fast extension and thinning of the lithosphere. Once the lithosphere is thinned, the variation of topography, thickness and density in such a lithosphere, subjected to a far field stress state, may have generated local extensional stress field [*Artyushkov*, 1973; *Fleitout and Froidevaux*, 1982]. This stress field overprinted the far field stress state, changing its direction and magnitude [*Sonder*, 1990]. The local extension was an extension perpendicular to the rift axis as it was induced perpendicular to the thinning, its direction was then around 160°E (Figure 11). The interaction between these local and far field extensions depends on their orientation and their magnitude [e.g., *Zoback*, 1992]. Here, the stress magnitudes are not known and do not allow us to calculate a direction for the resulting extension direction. However, it is obvious that this resulting extension was trending between the two extension directions (40° between 160°E and 020°E). This perturbed stress field can explain the 160°E to N-S extension measured in the Gulf of Aden margin [this study; *Huchon et al.*, 1991; *Khanbari*, 2000; *Lepvrier et al.*, 2002; *Huchon and Khanbari*, 2003; *Fournier et al.*, 2004]. *Huchon and Khanbari* [2003] discussed the origin of such an extensional phase, rejecting a change in plate motion origin and an oblique extension in transfer zones. They also reject an effect of the rift obliquity (during the rifting phase), arguing that many oblique rifts do not present such a late extensional phase. They prefer an explanation by a crack tip propagation model, where the oceanic ridge propagated toward the WSW under a 020°E extension, implying an extensional stress field whose extension was perpendicular (160°E) to the propagation. They, however, indicate that this hypothesis implies diachronism in this late extension (younger toward the WSW) and that this diachronism cannot be demonstrated in Yemen. We confirm that it cannot be shown in Oman, as already noted by *Lepvrier et al.* [2002]. Their model is then mostly constrained by the oceanic magnetic anomalies whose age is revised and identified as older

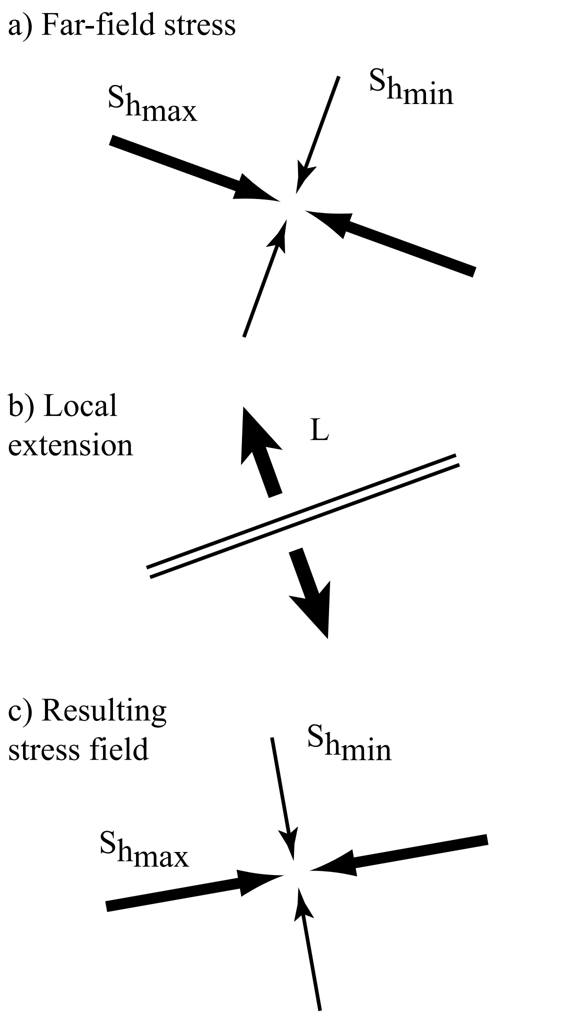

Figure 11. Possible stress field in the oblique rift of the Gulf of Aden, modified from *Sonder* [1990]. (a) Far-field stress state with an extension direction along the 020°E direction. (b) Rift zone that creates an extension (160°E) perpendicular to its axis (075°E). The combination of these two stress states result in a clockwise rotation of the extension to a direction between 020°E and 160°E depending on the stress magnitude (here unknown).

than previously determined by *Leroy et al.* [2004] and *d'Acremont et al.* [2006]. In the following, we present an alternative model based on lithospheric structural variations due to the rift obliquity as explained above.

4.4.2. Homogeneous Lithospheric Mantle

[36] If the lithospheric mantle is not weakened before the rifting, the way it will deform is then difficult to predict. There is precisely no strong argument for a preexisting lithospheric weakness with a 075°E orientation in the Gulf of Aden area. In such case, the obliquity between the rift axis and the direction of divergence can be due to the interaction of the boundary conditions in northeast Africa and the hot spot activity as shown by *Bellahsen et al.* [2003]. In such a case, several questions arise. How is this obliquity accommodated in the lithospheric mantle? It can be accommodated along a continuous zone of 075°E trend or it can be characterize by en échelon zones of deformation. If this is the case, what are the characteristic sizes (in plane view) of such zones? These questions could be only answered by testing this process in analogue and numerical models. However, we can speculate on the evolution of such a rift. In the Arabian crust, faults and basins are preexisting with an inherited distribution (Figure 12a). Once the rifting starts, during late Eocene and early Oligocene times, as the rift obliquity is not defined a priori, the extensional deformation in the crust and the reactivated basins should be extended as in an orthogonal rift. In this case, basins and 110°E striking faults are reactivated and other 110°E faults

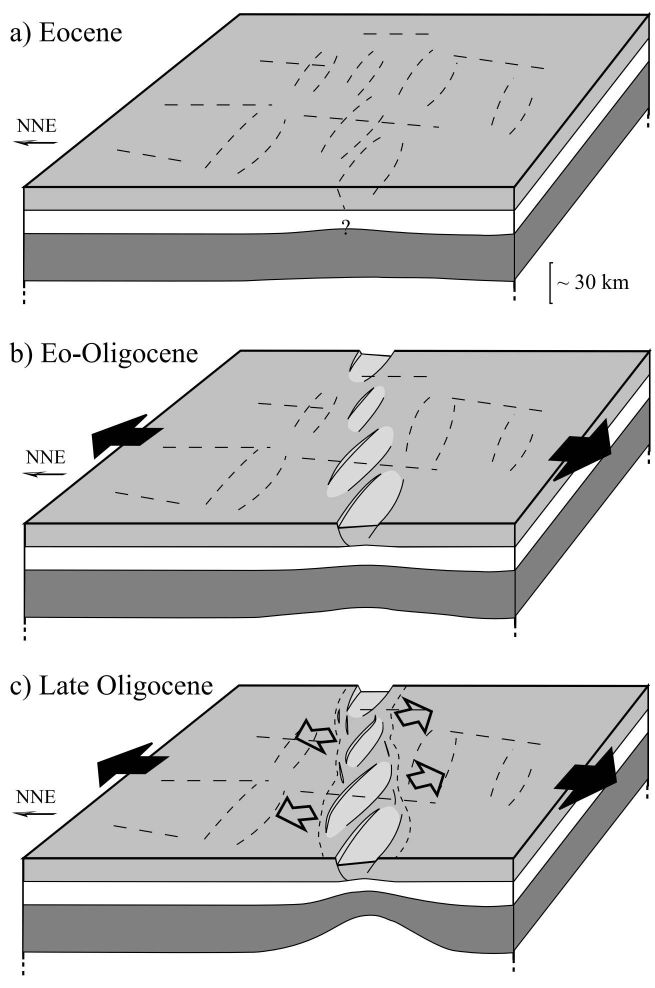

Figure 12. Model for the lithospheric evolution. (a) Eocene. Before rifting, Mesozoic basins are present in the Arabian crust. (b) At about 35 Ma. When the rifting starts, these basins are reactivated in a zone oblique to the extension direction. 110°E trending faults are reactivated and others are created to accommodate to extension. (c) With the rift evolution and its associated thinning during late Oligo-Miocene times. A clockwise rotation of the extension direction reactivated some 110°E striking faults and created some 070°E striking faults to produce the observed fault patterns.

are initiated in the eastern Gulf of Aden (Figure 12b). The rift direction is oblique to the divergence as explained earlier. During the rift localization process (Figure 12c), the rift obliquity tends to establish and can lead to stress rotation as suggested above (section 4.4.1). The thickness variations in the lithosphere can then create the 160°E extension that is, in this last model, clearly a late extension as it is due to the obliquity and tends to form in the late mature oblique rift. The extensional phase obliquely reactivated 110°E striking faults and creates new 070°E faults with geometries described in the analogue models presented in the previous sections.

[37] This model is significantly different than those of *Courtillot et al.* [1987], *Manighetti et al.* [1997] and *Hubert-Ferrari et al.* [2003]. They propose a model of rift propagation in a homogeneous lithosphere. While we agree with the homogeneous lithosphere idea, we think that rift propagation is not necessary to obtain the observed geometries and kinematics. Moreover, the propagation is not strongly supported by the stratigraphic data in the Gulf of Aden. However, *Huchon and Khanbari* [2003] also proposed a model of propagation based on stress field rotation. We interpret these stress field rotation as the consequence of the evolution of the lithosphere in a context of oblique rifting as explained above. Furthermore, we would like to point out that the rift axis-parallel faults (070°E in the Gulf of Aden) in oblique rift are due to such a mechanism and that their origin is related to the lithosphere evolution. *Tuckwell et al.* [1998] pointed out such relation in the case of oblique spreading center at oceanic ridges. In this context, the faults formed at the ridge axis are subperpendicular to the plate divergence and, when translated on the ridge shoulder, they undergo a different stress field guided by the lithospheric variations and whose extension is perpendicular to the ridge axis.

[38] However, the 3-D lithospheric deformation is not well constrained and several causes and consequences of rift direction origin and the inherited basins are still not well understood. In particular, what are the consequences of an oblique rifting not induced by a "linear (in plane view)" preexisting lithospheric discontinuity, in terms of normal faults geometry and evolution, possibility and characteristics of a mantle exhumation, and structure of the initial accretion segments? In other words, what happens when the heterogeneities are located, not in the lithospheric mantle, but in the crust?

5. Conclusions

[39] Field data, in the Gulf of Aden, show that a heterogeneous stress field was active during rifting, with possibly stress rotations. Moreover, the normal fault network geometry is complex, presenting several fault populations. These characteristics are not totally predicted by crustal analogue models of oblique rifting. New field data and analogue models of oblique reactivation, compared in this study, show that reactivation is an important process during rifting. All these observations lead us to build a model for the development of the Gulf of Aden: the rift localizes in an oblique zone (in response to the interaction of the Arabian boundary conditions and the Afar hot spot). In this zone, preexisting Mesozoic basins are reactivated and their disposition is, of course, inherited and different than the disposition obtained if the crust was homogeneous before the rifting. As the deformation continues, the rift localizes and lithospheric thinning generates a local extension perpendicular to that thinning, i.e., perpendicular to the rift, in a direction around 160° that can induce anticlockwise stress rotation. This extension, measured in the field, reactivated earlier faults (especially 110°E ones).

[40] However, to confirm, constrain or correct this model, we need lithospheric analogue and numerical models, in a 3-D configuration and with rheological constrains. Such models could constrain the way the lithosphere deforms and, in particular, the lithospheric upper mantle in a context of oblique rifting, where the rift axis is not an inherited zone of weakness.

[41] **Acknowledgments.** This work benefited from discussions and field work with Laurent Maerten and discussions with Claudio Faccenna. We thank Hilal Al-Azri for his help and the collaboration with the Directorate of Minerals of Sultanate of Oman. We would like to thank R. W. Schlische, N. Dawers, K. Khanbari, and E. Kirby for constructive comments. The GDR Marges and the Institut Français du Pétrole provided financial support. Contribution GDRMarges 2052.

References

Al-Husseini, M. I. (2000), Origin of the arabian plate structures: Amar collision and Nadj Rift, *GeoArabia*, *5*, 527–542.
Angelier, J. (1984), Tectonic analysis of fault slip data sets, *J. Geophys. Res.*, *89*, 5835–5848.
Angelier, J. (1989), From orientations to magnitudes in paleostress determinations using fault slip data, *J. Struct. Geol.*, *11*, 37–50.
Angelier, J. (1990), Inversion of field data in fault tectonics to obtain the regional stress III, A new rapid direct inversion method by analytical means, *Geophys. J. Int.*, *103*, 363–376.
Artyushkov, E. V. (1973), Stresses in the lithosphere caused by crustal thickness inhomogeneities, *J. Geophys. Res.*, *78*, 7675–7708.
Bellahsen, N., and J. M. Daniel (2005), Fault reactivation control on normal fault growth: An experimental study, *J. Struct. Geol.*, *27*, 769–780.
Bellahsen, N., C. Faccenna, F. Funiciello, J. M. Daniel, and L. Jolivet (2003), Why did Arabia separate from Africa? Insights from 3-D laboratory experiments, *Earth Planet. Sci. Lett.*, *216*, 365–381.
Berhe, S. M. (1986), Geologic and geochronologic constraints on the evolution of the Red Sea-Gulf of Aden and Afar Depression, *J. Afr. Earth Sci.*, *5*, 101–117.
Beydoun, Z. R., M. L. As-Sasuri, and R. S. Baraba (1996), Sedimentary basins of the Republic of Yemen: Their structural evolution and geological characteristics, *Oil Gas Sci. Technol.*, *51*, 763–775.
Birse, A. C. R., W. F. Bott, J. Morrison, and M. A. Samuel (1997), The Mesozoic and early Tertiary tectonic evolution of the Socotra area, eastern Gulf of Aden, Yemen, *Mar. Pet. Geol.*, *14*, 675–684.
Bosence, D. W. J. (1997), Mesozoic rift basins of Yemen, *Mar. Pet. Geol.*, *14*, 611–616.
Brun, J. P. (1999), Narrow rifts versus wide rifts: Inferences of rifting from laboratory experiments, *Philos. Trans. R. Soc. London*, *357*, 695–712.
Brun, J. P., and V. Tron (1993), Development of the North Viking Graben: Inferences from laboratory modelling, *Sediment. Geol.*, *86*, 31–51.
Clifton, A. E., R. W. Schlische, M. O. Withjack, and R. V. Ackermann (2000), Influence of rift obliquity on fault-population systematics: Results of experimental clay models, *J. Struct. Geol.*, *22*, 1491–1509.
Courtillot, V. (1980), Opening of the Gulf of Aden and Afar by progressive tearing, *Phys. Earth Planet. Inter.*, *21*, 343–350.
Courtillot, V., R. Armijo, and P. Tapponnier (1987), Kinematics of the Sinai triple junction and a two-phase model of Arabia-Africa rifting, in *Continental Extensional Tectonics*, edited by M. P. Coward,

J. F. Dewey and P. L. Hancock, *Geol. Soc. Spec. Publ.*, *28*, 559–573.
Courtillot, V., C. Jaupart, I. Manighetti, P. Tapponnier, and J. Besse (1999), On causal links between flood basalt and continental breakup, *Earth Planet. Sci. Lett.*, *166*, 177–195.
d'Acremont, E. (2002), De la déchirure continentale à l'accrétion océanique: Ouverture du golfe d'Aden, 330 pp., Univ. Pierre et Marie Curie, Paris.
d'Acremont, E., S. Leroy, M. O. Beslier, N. Bellahsen, M. Fournier, C. Robin, M. Maia, and P. Gente (2005), Structure and evolution of the eastern Gulf of Aden conjugate margins from seismic reflection data, *Geophys. J. Int.*, *160*, 869–890, doi:10.1111/j.1365-246X.2005.02524.
d'Acremont, E., S. Leroy, M. Maia, P. Patriat, M.-O. Beslier, N. Bellahsen, M. Fournier, and P. Gente (2006), Structure and evolution of the eastern Gulf of Aden: Insights from magnetic and gravity data (Encens-Sheba cruise), *Geophys. J. Int.*, in press.
Dauteuil, O., and J. P. Brun (1993), Oblique rifting in a slow-spreading ridge, *Nature*, *361*, 145–148.
Dauteuil, O., P. Huchon, F. Quemeneur, and T. Souriot (2001), Propagation of an oblique spreading centre: The western Gulf of Aden, *Tectonophysics*, *332*, 423–442.
Davy, P., and P. R. Cobbold (1991), Experiments on shortening of a 4–layer model on the continental lithosphere, *Tectonophysics*, *188*, 1–25.
Ellis, A. C., H. M. Kerr, C. P. Cornwell, and D. O. Williams (1996), A tectono-stratigraphic framework for Yemen and its implications for hydrocarbon potential, *Petroleum Geoscience*, *2*, 29–42.
Faerseth, R. B., B. E. knudsen, T. Liljedahl, P. S. Midboe, and B. Soderstrom (1997), Oblique rifting and sequential faulting in the Jurassic development of the northern North Sea, *J. Struct. Geol.*, *19*, 1285–1302.
Fantozzi, P. L., and M. Sgavetti (1998), Tectonic and sedimentary evolution of the eastern Gulf of Aden continental margins: New structural and stratigraphic data from Somalia and Yemen, in *Sedimentation and Tectonics of Rift Basins: Red Sea-Gulf of Aden*, edited by B. H. Purser and D. W. J. Bosence, pp. 56–76, CRC Press, Boca Raton, Fla.
Fleitout, L., and C. Froidevaux (1982), Tectonics and topography for a lithosphere containing density heterogeneities, *Tectonics*, *1*, 21–56.
Fournier, M., P. Patriat, and S. Leroy (2001), Reappraisal of the Arabia-India-Somalia triple junction kinematics, *Earth Planet. Sci. Lett.*, *189*, 103–114.
Fournier, M., N. Bellahsen, O. Fabbri, and Y. Gunnell (2004), Oblique rifting and segmentation of the NE Gulf of Aden passive margin, *Geochem. Geophys.* Geosyst., 5, Q11005, doi:10.1029/2004GC000731.
Granath, J. W. (2001), The Nogal rift of northern Somalia: Gulf of Aden. Reactivation of a Mesozoic rift, in *Peri-Tethys Memoir 6: Peri-Tethyan Rifts/Wrench Basins and Passive Margins*, edited by P. A. Ziegler et al., *Mem. Mus. Nat. Hist.*, *186*, 511–527.
Hubbert, M. K. (1937), Theory of scale models as applied to the study of geologic structures, *Geol. Soc. Am. Bull.*, *48*, 1459–1520.
Hubert-Ferrari, A., G. King, I. Manighetti, R. Armijo, B. Meyer, and P. Tapponnier (2003), Long-term elasticity in the continental lithosphere; modelling the Aden Ridge propagation and the Anatolian extrusion process, *Geophys. J. Int.*, *153*, 111–132.
Huchon, P., and K. Khanbari (2003), Rotation of the syn-rift stress field of the northern Gulf of Aden margin, Yemen, *Tectonophysics*, *364*, 147–166.
Huchon, P., F. Jestin, J. M. Cantagrel, J. M. Gaulier, S. A. Khirbash, and A. Gafaneh (1991), Extensional deformation in Yemen since Oligocene and the Africa-Arabia-Somalia triple junction, *Ann. Tectonicae*, *5*, 141–163.
Jestin, F., P. Huchon, and J. M. Gaulier (1994), The Somalia plate and the East African Rift System: Present-day kinematics, *Geophys. J. Int.*, *116*, 637–654.
Jolivet, L., and C. Faccenna (2000), Mediterranean extension and the Africa-Eurasia collision, *Tectonics*, *19*, 1095–1106.
Katz, M. B. (1987), East African rift and northeast lineaments; continental spreading-transform system?, *J. Afr. Earth Sci.*, *6*, 103–107.
Khanbari, K. (2000), Propagation d'un rift océanique: Le Golfe d'Aden. Ses effets structuraux sur la marge yéménite, 221 pp., Univ. Paris-Sud, Paris.
Lepvrier, C., M. Fournier, T. Berard, and J. Roger (2002), Cenozoic extension in coastal Dhofar (southern Oman): Implications on the oblique rifting of the Gulf of Aden, *Tectonophysics*, *357*, 279–293.
Leroy, S., et al. (2004), From rifting to drifting in the eastern Gulf of Aden: A complete survey coverage of a young oceanic basin from margin to margin, *Terra Nova*, *16*, 185–192, doi:10.1111/j.1365-3121.2004.00550.
Manighetti, I., P. Tapponnier, V. Courtillot, S. Gruszow, and P. Y. Gillot (1997), Propagation of rifting along the Arabia-Somalia plate boundary: The gulfs of Aden and Tadjoura, *J. Geophys. Res.*, *102*, 2681–2710.
Manighetti, I., P. Tapponnier, P. Y. Gillot, E. Jacques, V. Courtillot, R. Armijo, J. C. Ruegg, and G. King (1998), Propagation of rifting along the Arabia-Somalia plate boundary: Into Afar, *J. Geophys. Res.*, *103*, 4947–4974.
McClay, K. R., and M. J. White (1995), Analogue modelling of orthogonal and oblique rifting, *Mar. Pet. Geol.*, *12*, 137–151.
Morgan, W. J. (1983), Hotspots tracks and the early rifting of the Atlantic, *Tectonophysics*, *94*, 123–139.
Platel, J. P., and J. Roger (1989), Evolution géodynamique du Dhofar (Sultanat d'Oman) pendant le Crétacé et le Tertiaire en relation avec l'ouverture du golfe d'Aden, *Bull. Soc. Geol. Fr.*, *5*, 253–263.
Roger, J., J. P. Platel, C. Cavelier, and C. B. D. Grisac (1989), Données nouvelles sur la stratigraphie et l'histoire géologique du Dhofar (Sultanat d'Oman), *Bull. Soc. Geol. Fr.*, *5*, 265–277.
Schlische, R. W., M. O. Withjack, and G. Eisenstadt (2002), An experimental study of the secondary deformation produced by oblique-slip normal faulting, *AAPG Bull.*, *86*, 885–906.
Sonder, L. J. (1990), Effects of density contrasts on the orientation of stresses in the lithosphere: Relation to principal stress directions in the Transverse Ranges, California, *Tectonics*, *9*, 761–771.
Tron, V., and J. P. Brun (1991), Experiments on oblique rifting in brittle-ductile systems, *Tectonophysics*, *188*, 71–84.
Tuckwell, G. W., J. M. Bull, and D. J. Sanderson (1998), Numerical models of faulting at oblique spreading centers, *J. Geophys. Res.*, *103*, 15,474–15,482.
Watchorn, F., G. J. Nichols, and D. W. J. Bosence (1998), Rift related sedimentation and stratigraphy, southern Yemen (Gulf of Aden), in *Sedimentation and Tectonics of rift basins: Red Sea-Gulf of Aden*, edited by B. H. Purser and D. W. J. Bosence, pp. 165–189, CRC Press, Boca Raton, Fla.
Withjack, M. O., and W. R. Jamison (1986), Deformation produced by oblique rifting, *Tectonophysics*, *126*, 99–124.
Zoback, M. L. (1992), First- and second-order pattern of stress in the lithosphere: The World Stress Map Project, *J. Geophys. Res.*, *97*, 11,703–11,728.

N. Bellahsen, E. d'Acremont, M. Fournier, and S. Leroy, Laboratoire de Tectonique UMR 7072, Université Pierre et Marie Curie, T 46-00, E2, Case 129, 4 place Jussieu, F-75252 Paris cedex 05, France. (nicolas.bellahsen@lgs.jussieu.fr)

J. M. Daniel, Division Géologie-Géochimie, Institut Français du Pétrole, 1 et 4 av de bois Préau, F-92852 Rueil Malmaison, France.